HEP'99 # 1_225
Submitted to Pa 1, 3
Pl 1, 3

DELPHI 99-123 CONF 310
15 June 1999

Inclusive Spectra at 189 GeV

Preliminary

DELPHI Collaboration

Paper submitted to the HEP'99 Conference
Tampere, Finland, July 15-21

HEP'99 # 1_225
Submitted to Pa 1, 3
Pl 1, 3

DELPHI 99-123 CONF 310
15 June 1999

Inclusive Spectra at 189 GeV

Preliminary

DELPHI Collaboration

O.Passon [1] **J.Drees** [1], **K.Hamacher** [1],

Abstract

Inclusive charged hadron distributions from the DELPHI measurement at 189 GeV are presented as a function of the variables rapidity, ξ_p, p and transverse momenta. Data are compared with event generators and with calculations in the framework of the Modified Leading Logarithmic Approximation (MLLA), in order to examine the hypothesis of local parton hadron duality (LPHD).

Paper submitted to the HEP'99 Conference
Tampere, Finnland, July 15-21

[1] Fachbereich Physik, Bergische Universität-GH Wuppertal Gaußstraße 20, 42097 Wuppertal, Germany

1 Introduction

This paper presents inclusive charged hadron spectra measured by DELPHI at a centre-of-mass energy of 189 GeV. The results are compared to previous Z and LEP2 data and to measurements from lower energies. It is an update of the analysis [1], which might be consulted for further details.

Inclusive stable hadron spectra are highly sensitive to properties of the hadronization process and to resonance decays as well as to details of the parton shower. They depend on the amount of large angle and collinear gluon radiation and on the coherence of gluon radiation. The measurements therefore provide rigid constraints on models of the hadronization process.

Direct comparisons of inclusive distributions with QCD calculations suffer from their dependence on infrared and collinear divergences: finite predictions in the framework of perturbative QCD can only be obtained by introducing a cut-off in momentum. Moreover, to compare calculations of spectra to experimental data one has to assume that parton distributions are proportional to inclusive hadron distributions; this is frequently referred to as "local parton hadron duality" (LPHD) [2].

In Section 2 the selection of hadronic events, the reconstruction of the centre-of-mass energy, the correction procedures applied to the data and especially the corrections for the background from W^+W^- events are briefly discussed. In Section 3 the inclusive spectra as measured by DELPHI are compared with the predictions from different Monte Carlo models. Results concerning the energy dependence of the distributions of scaled and absolute momenta are presented. A brief summary is given in Section 4 .

2 Selection and correction of hadronic data

The analysis is based on data taken with the DELPHI detector at 189 GeV. The integrated luminosity corresponds to about $157\,\mathrm{pb}^{-1}$.

DELPHI is a hermetic detector with a solenoidal magnetic field of 1.2 T. The tracking detectors, which lie in front of the electromagnetic calorimeters, are a silicon micro vertex detector VD, a combined jet/proportional chamber inner detector ID, a time projection chamber TPC as the major tracking device, and the streamer tube outer detector OD in the barrel region. The forward region is covered by the drift chamber detectors FCA and FCB.

The electromagnetic calorimeters are the high density projection chamber HPC in the barrel, the lead glass calorimeter FEMC in the forward region and the STIC next to the beam pipe. Detailed information about the construction and performance of DELPHI can be found in [3, 4]. The standard system of coordinates of DELPHI is also defined in [4].

In order to select well measured charged particle tracks, the cuts given in the upper part of Table 1 have been applied. The cuts in the lower part of the table have been used to select hadronic events $e^+e^- \to \mathrm{Z}/\gamma \to q\bar{q}$ and to suppress background processes such as two photon interactions, beam gas and beam wall interactions, leptonic final states, and, most important for the LEP2 analysis, events with large initial state radiation (ISR) and W pair production. At energies above the Z peak, initial fermions may radiate one or more photons before they interact, such that the effective centre-of-mass energy for the collision

track selection	
p[GeV]	$0.2 \leq p \leq 100$
$\Delta p/p$	≤ 1
θ	$20^\circ \leq \theta \leq 160^\circ$
track length	≥ 30cm
$\Delta_{r\phi}$	≤ 4cm
Δ_z	≤ 10cm
event selection	
$\theta_{\rm Thrust}$	$25^\circ \leq \theta \leq 155^\circ$
$E_{\rm tot}$	$\geq 50\%\ E_{CM}$
$\sqrt{s'}$	$\geq 90\%\ E_{CM}$
$N_{\rm ch}$	$42 \geq \mathrm{N}_{ch} \geq 7$
$B_{\rm min}$	≤ 0.08

Table 1: Selection of charged particles and events. p is the momentum, θ is the polar angle with respect to the beam (likewise $\theta_{\rm Thrust}$ for the thrust axis $n_{\rm T}$), $\Delta_{r\phi}$ and Δ_z are the distances to the interaction point in $r\phi$ (radial distance to beam axis and azimuthal angle) and z (distance along the beam axis) respectively. $N_{\rm ch}$ is the number of charged particles, $E_{\rm tot}$ the total energy carried by all selected particles, s' the square of the reconstructed centre-of-mass energy, reduced by initial state radiation. $E_{\rm CM}$ is the nominal LEP energy, $B_{\rm min}$ is the minimal jet broadening (see text).

is the mass of the Z. These "radiative return events" are the dominant part of the cross–section. The initial state radiation (ISR) is typically aligned along the beam direction and the photons are only rarely identified inside the detector. In order to evaluate the effective centre-of-mass energy ($\sqrt{s'}$) of an event, considering ISR, an algorithm is used that is based on a constrained fit method using four–momenta of jets and taking energy and momentum conservation into account [6].

The production of W pairs occurs above the threshold of 161 GeV . Since the topological signatures of QCD four–jet events and hadronic WW events (and other four fermion background) are very similar, no highly efficient separation of the two classes of events is possible. As a suitable discriminant variable for performing the separation the shape $B_{\rm min}$ is chosen, which is defined as $B_{\rm min} = \min\{B_+, B_-\}$ with:

$$B_\pm = \frac{\sum_{\pm\vec{p}_i \cdot \hat{n}_{\rm T} > 0} |\vec{p}_i \times \hat{n}_{\rm T}|}{2 \sum |\vec{p}_i|} ,$$

where the sum runs over all selected particles. The cut applied to the maximum charged multiplicity also discards W events. The event selection cuts (table 1) are optimized in order to maximize the purity with respect to the $\sqrt{s'}$ selection, the efficiency of collecting high energy $q\bar{q}$ events and the WW rejection. Furthermore the QCD bias introduced by the $B_{\rm min}$ cut is minimized. Table 2 shows the efficiency of the WW rejection and the remaining contamination. This WW contribution was evaluated by Monte Carlo simulation and subtracted from the data. The small effect of Z pair production was also taken into account. Two photon events are strongly suppressed by the cuts. Leptonic background can also be neglected in this analysis.

	189 GeV
$\mathcal{L}$	156.6 pb^{-1}
$\sigma_{q\bar{q}}$	99.8 pb
$\sigma_{q\bar{q}}$ $(\sqrt{s'} > 0.9 \cdot \sqrt{s})$	18.2 pb
$\sqrt{s'}$ purity	0.94
σ_{WW}	16.65 pb
WW rejection efficiency	0.81
WW background events	477
σ_{ZZ}	1.59 pb
ZZ rejection efficiency	0.84
ZZ background events	41
selected events	3382

Table 2: Integrated luminosity, cross– sections of quark, Z and W pair production, efficiency of rejecting the last two event classes, and number of remaining background events. These are subtracted assuming the background to be distributed as in the simulation. Monte Carlo studies demonstrate that other background sources give negligible contributions. The last row shows the number of *selected* hadronic events (including background).

The influence of detector effects was studied by passing generated events (PYTHIA[5] tuned by DELPHI [7]) through the full detector simulation (DELSIM [4]). Such simulated events were processed with the same cuts as real data. They are identified by the subscipt "acc" in the following. The tuned generator prediction is denoted as "gen". In order to correct for cuts, detector and ISR effects, a bin by bin correction factor (acceptance correction) was applied to the data. For bin f of histogram h it is defined as:

$$C = \frac{h(f)_{\mathrm{gen,noISR}}}{h(f)_{\mathrm{acc}}} \,. \tag{1}$$

For $h(f)_{\mathrm{acc}}$ all cuts were applied, for $h(f)_{\mathrm{gen,noISR}}$ a total ISR of less than 1 GeV was demanded.

3 Results

Comparisons of inclusive distributions with model expectations are presented as a function of the logarithm of the scaled hadron momentum $\xi_p = \ln(1/x_p)$ (with $x_p = p/p_{\mathrm{beam}}$), the rapidity with respect to the thrust axis $y_t = 0.5 \cdot \ln((E + p_{\parallel})/(E - p_{\parallel}))$ as well as the two momentum components (p_t^{in}, p_t^{out}) transverse to the thrust axis which lie in and perpendicular to the plane of the event. E and p are the particle momenta and energies respectively. All energies have been computed assuming the charged particles to be pions, and the momenta of neutral particles assuming them to be massless.

Figures 1 show the ξ_p, y_t, p_t^{in} and p_t^{out} spectra as determined from the 189 GeV data. The data are compared to the JETSET 7.4, HERWIG 5.8 and ARIADNE 4.08 fragmentation models as tuned by DELPHI [7]. The shaded areas display the size of the

WW and ZZ background which was subtracted from the data. The upper inset in these plots shows the correction factor applied to the data. The lower inset presents the ratio of the high energy data to the corresponding results at the Z. This ratio is again compared to the model predictions.

The models describe well all inclusive spectra measured at the high energy and also the energy evolution from the Z peak (see the lower inset of Fig. 1). The most prominent change in the ξ_p distribution (Fig. 1 a) is an increase at large ξ_p (i.e. low x_p). In the rapidity distribution (Fig. 1 b) the expected increase of the width of the distribution is clearly observed together with a slight increase of the plateau height. These changes and the strong increase in the transverse momentum distributions at large $p_\perp$ (Fig. 1 d) are due to stronger gluon radiation at the higher energies.

3.1 Energy Dependence of ξ_p and ξ^*

The shape of the partonic ξ_p distribution, as calculated in the Modified Leading Log Approximation (MLLA), exhibits the characteristic "hump backed" plateau due to suppression of soft gluon radiation [18]. The calculation in the "limited spectrum" approximation ($\Lambda_{\rm eff} = Q_0$) can be well expressed by a distorted Gaussian (2):

$$\frac{1}{N_{\rm event}}\frac{dn}{d\xi_p} = \frac{N(Y)}{\sigma\sqrt{2\pi}}\exp\left(\frac{k}{8} - \frac{s\delta}{2} - \frac{(2+k)\delta^2}{4} + \frac{s\delta^3}{6} + \frac{k\delta^4}{24}\right) \tag{2}$$

with $\delta = (\xi - <\xi>)/(\sigma)$, $<\xi>$ the mean, σ the width, s the skewness and k the kurtosis of the distribution. $N(Y)$ is an energy dependent normalization factor. With the number of participating quark flavours, N_F, $\beta = 11 - 2N_F/3$, $\rho = 11 + 2N_F/27$ and $\omega = 1 + N_F/27$ one obtains for *quark jets* [19]:

$$\begin{aligned}
<\xi> &= \frac{1}{2}Y\cdot\left(1+\frac{\rho}{24}\sqrt{\frac{48}{\beta Y}}\right)\cdot\left(1-\frac{\omega}{6Y}\right)+\mathcal{O}(1)\\
\sigma &= \sqrt{\frac{Y}{3}}\cdot\left(\frac{\beta Y}{48}\right)^{1/4}\cdot\left(1-\frac{\beta}{64}\sqrt{\frac{48}{\beta Y}}\right)\cdot\left(1+\frac{\omega}{8Y}\right)+\mathcal{O}(Y^{-1/4})\\
s &= -\frac{\rho}{16}\sqrt{\frac{3}{Y}}\cdot\left(\frac{48}{\beta Y}\right)^{1/4}\cdot\left(1+\frac{\omega}{4Y}\right)+\mathcal{O}(Y^{-5/4})\\
k &= -\frac{27}{5Y}\cdot\left(\sqrt{\frac{\beta Y}{48}}-\frac{\beta}{24}\right)\cdot\left(1+\frac{5\omega}{12Y}\right)+\mathcal{O}(Y^{-3/2})
\end{aligned}$$

Here $Y = \ln(E_{\rm beam}/\Lambda_{\rm eff})$ and $\Lambda_{\rm eff}$ is an effective scale parameter. $\Lambda_{\rm eff}$, the overall normalization N and the additional constant term of $\mathcal{O}(1)$ in $<\xi>$ are the free parameters in this expression which is valid in the region around the maximum, and contains high energy approximations. Using the Local Parton Hadron Duality (LPHD) hypothesis this shape can directly be adapted to the measured hadron spectrum [2]. In Fig. 2 the ξ_p distributions as determined from LEP2 data are compared to the DELPHI results at the Z [7] and to other experiments [13, 20]. The full lines are the results of a simultaneous fit of the Fong-Webber parametrisation (2) to all but the Z data yielding χ^2/dof=99.6/97. The Z data are left out because of the higher rate of $b\bar{b}$ events included in this sample, which leads to a shift of the maximum of the ξ distribution, ξ^*, to smaller values. Values

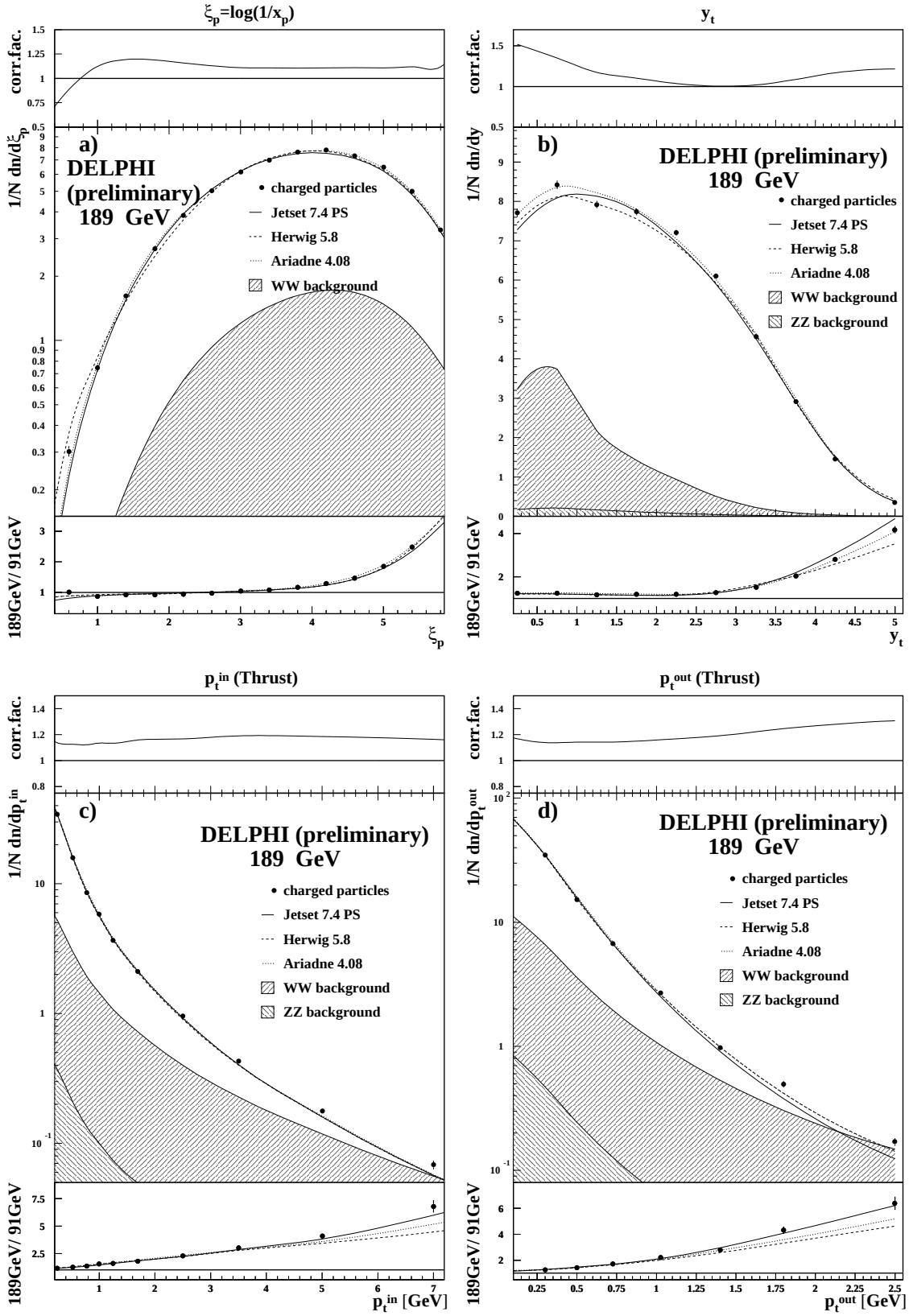

Figure 1: inclusive spectra at 189 GeV. The shaded areas display the WW – respectively ZZ background which has been subtracted from the data. The upper insets in these plots show the correction factor applied to the data. The lower insets present the ratio of the high energy data to the corresponding results at the Z.

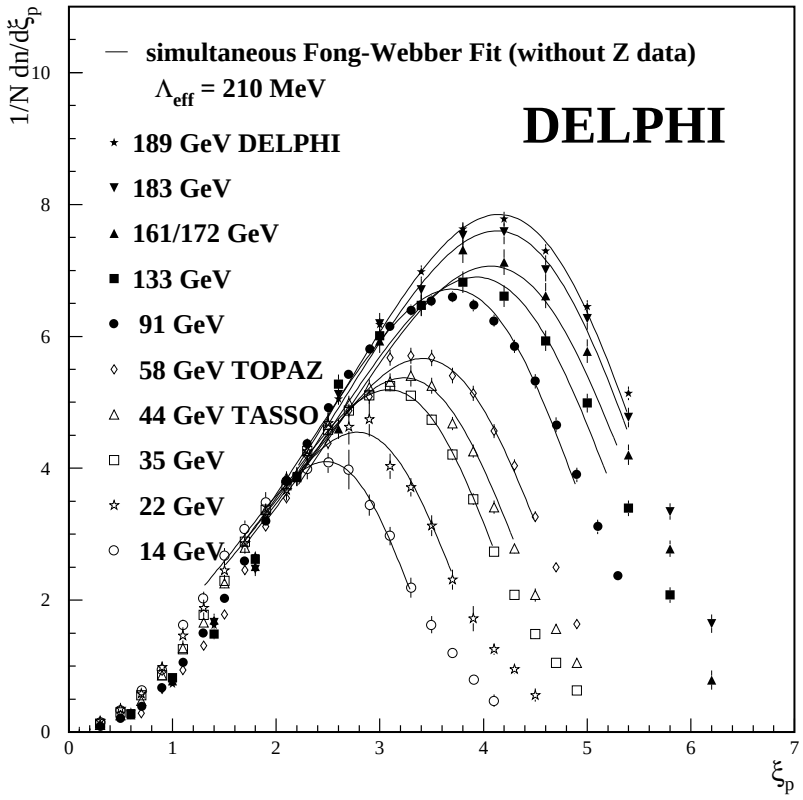

Figure 2: ξ_p distributions for charged particles. The full lines present the results of a simultaneous fit of the Fong-Webber parametrisation (2). The curves are drawn over the range of the fit ($\approx 50\%$ of the maximum height).

of $\Lambda_{\rm eff} = 210 \pm 8$ MeV and -0.55 ± 0.03 for the $\mathcal{O}(1)$ correction to $< \xi >$ are obtained for the energy independent parameters. Here $N_F = 3$ was chosen since light quarks dominate quark pair production in the cascade.

MLLA also provides a definite prediction for the energy evolution of ξ^*. As hadronization and resonance decays are expected to act similarly at different centre-of-mass energies, the energy evolution of ξ^* is expected to be less sensitive to nonperturbative effects. A small correction is to be expected, however, due to varying contribution of heavy quark events. These chain decays are known to shift ξ^* in a way different from ordinary resonance decays. This shift also differs for the individual stable particle species due to their different masses. In this paper the influence of heavy decays is neglected.

The ξ^* values entering in this analysis were determined by fitting a distorted Gaussian with the parameters s, k, $< \xi >$ and σ given by the Fong-Webber calculation. The fit range in ξ is restricted to the part of the distribution close to the maximum with $1/\mathrm{N}\ \mathrm{dn}/\mathrm{d}\xi_p \geq 0.6\ (1/\mathrm{N}\ \mathrm{dn}/\mathrm{d}\xi_p)_{\max}$. To avoid systematic differences due to different strategies for the ξ^* determination, this fit has also been performed at the other energies [21, 22].

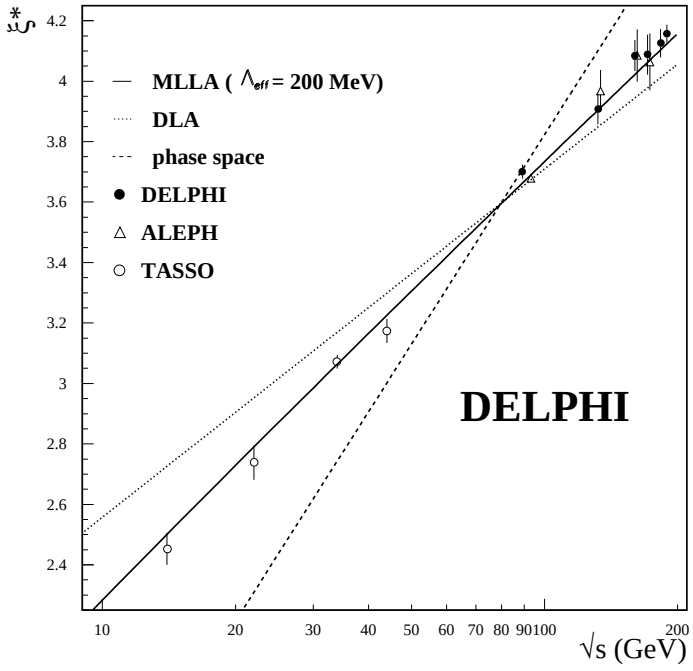

Figure 3: Energy evolution of the ξ_p peak position. $\Lambda_{\rm eff}$ is obtained from a fit to the MLLA/LPHD prediction. The phase space and DLA predictions are described in the text.

For the 189 GeV data one obtains $\xi^* = 4.157 \pm 0.030$, where the statistical and systematic error are added in quadrature. The full line in Fig. 3 shows a fit of the MLLA prediction

$$\xi^* = 0.5 \cdot Y + \sqrt{C} \cdot \sqrt{Y} - C + \mathcal{O}(Y^{-\frac{3}{2}}) \tag{3}$$

to the data.

From this fit $\Lambda_{\rm eff} = 200 \pm 2$ MeV. This is in good agreement with the $\Lambda_{\rm eff}$ value obtained from the fit to the whole spectra. The quantity $C = \frac{\rho^2}{48\beta}$ depends on the number of active flavours ($C(N_F = 3) = 0.2915$, $C(N_F = 5) = 0.3513$). The results are presented for $N_F = 3$. The dashed line in Fig. 3 represents the slope of the phase space expectation $\xi^* = a + Y$ [23]. Due to angular ordering of gluon bremsstrahlung the rise in ξ^* is slower in the MLLA prediction. The dotted line represents the fit of only the first term of equation 3, which is the result in the double logarithmic approximation (DLA).

3.2 Energy Dependence of the Momentum Distribution

As the scaled momentum distribution may veil effects connected to an absolute scale, the evolution of the differential cross–section in absolute momentum p is also of interest. In Fig. 4 a) the momentum spectra obtained for the different centre-of-mass energies and the corresponding predictions of the JETSET model are compared.

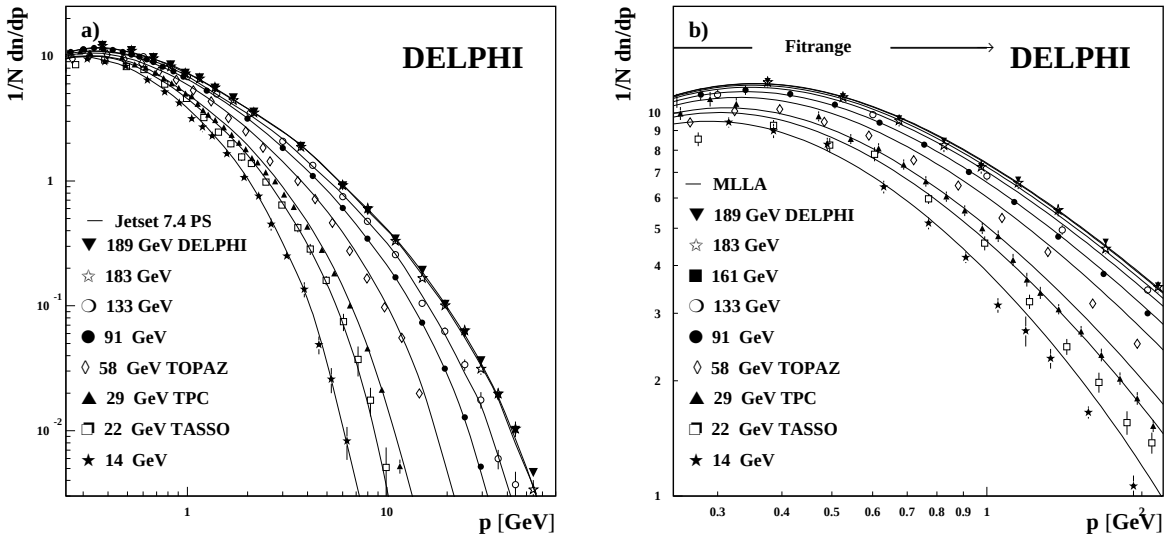

Figure 4: a) 1/N dn/dp distribution compared to JETSET for $p \leq 55$ GeV and b) to MLLA/LPHD prediction for $p \leq 2.5$ GeV. The parameter values of this fit are given in the last row of table 3

For the low energy and Z data the spectra are obtained by rescaling the x_p distribution [7, 13, 20, 25]. The energy evolution is well described by the fragmentation model. The most obvious feature is the increase of the distributions at large hadron momentum with energy. This is simply due to the enlarged phase space. A more interesting feature is the approximate $E_{\rm CM}$ independence of hadron production at very small momentum $p < 1$ GeV. This behaviour has been explained in [26] to be due to the coherent emission of low energy (i.e. long wavelength) gluons by the total colour current. This colour current is independent of the internal jet structure and conserved under parton splittings. Therefore low energy gluon emission is expected to be almost independent of the number of hard gluons radiated and hence of the centre-of-mass energy. As a consequence, the number of produced hadrons at small momentum is approximately constant.

In its range of validity ($p \leq 1$GeV) this prediction [26] is compared to the data in Fig. 4 b). It depends on the cutoff parameter Q_0, $\lambda = \log(Q_0/\Lambda_{\rm eff})$ and the normalisation K_H which relates parton and hadron distributions according to the LPHD hypothesis. It should be noted, that in contrast to the ξ_p calculations this prediction is *not* obtained in the "limited spectrum" ($\Lambda_{\rm eff} = Q_0$) approximation.

The curves in Fig. 4 b) correspond to a simultaneous fit of all DELPHI data from 91 to 189 GeV. Fitting all data or only the low energy data yields different values (especially in the logarithmic variable λ), but it should be noted that these parameters are highly correlated. Table 3 shows the different fit results. The large χ^2/dof for the fits of the low energy data compared to the satisfactory χ^2/dof for the DELPHI data may indicate systematic discrepancies between the measurements of the different experiments. Also the agreement with the MLLA/LPHD prediction is only expected to be qualitive, since many non-perturbative effects should be beyond its predictive power.

fitted energies [GeV]	Q_0 [MeV]	$\lambda = \log(Q_0/\Lambda_{\rm eff})$	K_H	χ^2/dof
low (14 - 58)	228 $\pm$ 4	0.055 $\pm$ 0.008	0.71 $\pm$ 0.04	118/34
DELPHI (91.2 - 189)	226 $\pm$ 3	0.020 $\pm$ 0.004	0.53 $\pm$ 0.04	17/26

Table 3: Parameters obtained from simultaneous fits of the LPHD/MLLA prediction to the momentum spectra at different energies.

4 Summary

Inclusive charged hadron distributions as obtained from the DELPHI measurement at 189 GeV are presented. Fragmentation models tuned at the Z describe the data well at higher energies. MLLA calculations in the limited spectrum approximation ($\Lambda_{\rm eff} = Q_0$) allow the ξ_p distribution and the energy dependence of its maximum to be parameterised. The calculation [26] for the soft part of the partonic momentum spectrum is able to describe the hadronic p distribution in the range of small momenta. All these measurements yield values for $\Lambda_{\rm eff}$ from 200 to 221 MeV. This supports the assumption of local parton hadron duality.

Acknowledgements

We thank W. Ochs for helpful discussions and S. Lupia for providing us with the code for the $\frac{dn}{dp}$ calculation.
We are greatly indebted to our technical collaborators, to the members of the CERN-SL Division for the excellent performance of the LEP collider, and to the funding agencies for their support in building and operating the DELPHI detector.

References

[1] DELPHI Coll., P. Abreu et al., CERN-EP 99-57 *accepted by Phys.Lett.B*

[2] Y. I. Azimov, Y. L. Dokshitzer, V. A. Khoze and S. I. Troyan, *Z. Phys.* **C27**(1985) 65.

[3] DELPHI Coll., P. Abreu et al., *Nucl. Instr. Meth.* **A303**(1991) 187.

[4] DELPHI Coll., P. Abreu et al., *Nucl. Instr. Meth.* **A378**(1996) 57.

[5] T. Sjöstrand, *Comp. Phys. Comm.* **39**(1986) 347.

[6] P. Abreu et al., "The Estimation of the Effective Centre of Mass Energy in $q\bar{q}\gamma$ Events from DELPHI", CERN-OPEN/98-026 (September 1998), submitted to Nucl. Instr. Methods A.

[7] DELPHI Coll., P. Abreu et al., *Z. Phys.* **C73**(1996) 11.

[8] TASSO Coll., W.Braunschweig et al., *Z.Phys.* **C41**(1988) 359.

[9] MARK II Coll., A.Petersen et al., *Phys.Rev.* **D37**(1988) 1.

[10] AMY Coll., Lie et al., *Phys.Rep.* **D41**(1990) 2675.

[11] TASSO Coll., M.Althoff et al., *Z.Phys.* **C22**(1984) 307.

[12] AMY Coll., H.Zheng et al., *Phys.Rev.* **D42**(1990) 737.

[13] TASSO Coll., W.Braunschweig et al., *Z. Phys.* **C47**(1990) 187.

[14] DELPHI Coll., P. Abreu et al., *Z. Phys.* **C 70**(1996) 179.

[15] DELPHI Coll., P. Abreu et al., *Phys. Lett.* **B 372**(1996) 172.

[16] DELPHI Coll., P. Abreu et al., *Phys. Lett.* **B 416**(1998) 233.

[17] DELPHI Coll., P. Abreu et al., Ref. #287 contributed to the ICHEP conference in Vancouver, 1998.

[18] Y. L. Dokshitzer, V. A. Khoze and S. I. Troyan, *Z. Phys.* **C55**(1992) 107.

[19] C. P. Fong and B. R. Webber, *Phys. Lett.* **B229**(1989) 289.

[20] TOPAZ Coll., R. Itoh et al., *Phys. Lett.* **B345**(1995) 335.

[21] ALEPH Coll., Ref. #629 contributed to the EPS HEP conference in Jerusalem, 1997.

[22] ALEPH Coll., R. Barate et al., *Phys.Rep.* **294**(1998) 1.

[23] B.R.Webber, Hadronization. Lectures at Summer School on Hadronic Aspects of Collider Physics, Zuoz, Switzerland, hep-ph/9411384, 1994.

[24] Y.L.Dokshitzer, V.A.Khoze, C.P.Fong and B.R.Webber, *Phys.Lett.* **B273**(1991) 319.

[25] TPC/2γ Coll., Aihara et al., *Phys. Rev. Lett.* **61**(1988) 1263.

[26] V. Khoze, S. Lupia and W. Ochs, *Phys. Lett.* **B394**(1997) 179.